

Exchange and correlation effects beyond the LDA on the dielectric function of silicon

Valerio Olevano, Maurizia Palumbo, Giovanni Onida, and Rodolfo Del Sole

*Istituto Nazionale per la Fisica della Materia - Dipartimento di Fisica dell' Università di Roma "Tor Vergata,"
Via della Ricerca Scientifica 1, I-00133 Roma, Italy*

(Received 25 March 1999)

The macroscopic dielectric function of crystalline silicon is calculated within density-functional theory, considering exchange and correlation effects beyond the local-density approximation. Reproposing an original idea of Hohenberg and Kohn, we consider a functional based on the exchange and correlation kernel of the homogeneous electron gas, K_{xc}^{HEG} . The same kernel is used in the evaluation of the dielectric matrix, keeping local-field effects into account. The results, compared with those obtained in the local-density approximation, show a limited reduction of the well-known overestimation of the macroscopic dielectric constant. Results obtained for optical and energy loss spectra are also presented. [S0163-1829(99)00344-6]

I. INTRODUCTION

Density-functional theory¹⁻³ provides a formally exact tool for the description of all the ground-state properties of many-electron systems at zero temperature, starting from first principles. The only essential approximation introduced in actual calculations is in the exchange-correlation term of the energy functional, since its exact form is unknown. The most widely used expression for the exchange-correlation functional is obtained in the local-density approximation (LDA),³ which, over the past 20 years, has been shown to yield results for crystal structures, lattice constants, elastic constants, and phonon frequencies within a few percent from the experiment, for a wide class of materials.^{4,5}

A remarkable exception is the static macroscopic dielectric constant ϵ_M , whose value is substantially overestimated by density-functional theory (DFT) LDA.⁶⁻⁸ The exact amount of such an overestimate depends on the lattice constant used in the calculation (and on other factors as pseudo-potential types, basis sets, etc.) but it ranges always between 12% and 18%.

This point deserves an accurate discussion. The macroscopic dielectric constant of a system is related to the change in the electronic ground state induced by an external perturbing electrostatic potential δV_{ext} . Since, within DFT, the ground-state density ρ can be computed (at least in principle) exactly, for both the unperturbed and perturbed systems, the difference $\delta\rho = (\rho_{pert} - \rho_0)$ can also be obtained exactly. Hence, treating adequately the variation of the external potential (either by a direct approach or by using perturbation theory), the dielectric constant should come out correctly within DFT. The large discrepancy with the experiments seems hence to be uniquely due to the LDA. However, it has been recently argued that this is not necessarily true.⁹⁻¹¹ On the other hand, Levine and Allan¹² performed calculations of ϵ_M within a quasiparticle scheme, i.e., in the framework of an excited-state theory. They obtained a value of ϵ_M for Silicon within 3% from experiment. However, as pointed out by Dal Corso, Baroni, and Resta,¹³ there is no immediate justification for the failure of DFT.

The question why DFT-LDA is unable to reproduce the experimental macroscopic dielectric constant was recently

faced by Gonze, Ghosez, and Godby (GGG).⁹⁻¹¹ They argued that the Hohenberg-Kohn theorem in its original form does not apply to the case of an infinite, periodic, nonmetallic system in the presence of a long-wavelength perturbation. The ground-state energy is not, in this case, a unique functional of the density. Rather, GGG demonstrated the appearance of a dependence of the exchange-correlation functional on the *macroscopic polarization* of the sample, \mathbf{P}_{mac} . GGG, hence, were lead to introduce a density-polarization functional theory (DPFT), extending the scheme of the traditional DFT. This problem has been studied in detail also by Resta,^{14,15} and by Martin and Ortiz.¹⁶⁻¹⁸ The latter have recently shown that, even if for zero external field a symmetric crystal is described by the usual density-only Kohn-Sham equations, the dependence of the exchange-correlation energy upon \mathbf{P}_{mac} can influence the dielectric properties of the system.¹⁸ Aulbur, Jönsson and Wilkins¹⁹ studied the implications of such a polarization dependence. Developing an original idea of Gonze, Ghosez, and Godby, they have shown how, in some cases, substituting the DFT eigenvalues with true quasiparticle energies (i.e., considering self-energy corrections) turns out to be an approximate way to include the effects of the polarization. Hence, the use of a scissor operator, as formerly proposed by Levine and Allan, has been justified *a posteriori*, and can be considered as a way to account for the polarization dependence.²⁰

Unfortunately, no approximation for the polarization dependence of the exchange-correlation energy functional is available at the moment. Hence, the problem of DPFT will not be addressed in the present work; instead, our aim is to investigate, *within DFT*, how much of the error on the dielectric constant is due to LDA, i.e., is not intrinsic to DFT. Our main reference is the work of Dal Corso, Baroni, and Resta,¹³ where ϵ_M was computed overcoming the LDA through the scheme of the generalized gradient corrections approximation (GGA).^{21,22} The main success of the GGA is a definite improvement of cohesive energies in molecules and solids. However, the improvement on other physical quantities is not so striking; in some cases, like for lattice constants and bulk moduli, the GGA even leads to a worsening.²³⁻²⁷ On the other hand, it can be said that the GGA is aimed at systems of slowly varying density, and (as

for the LDA) its application to systems with large density gradients is not justified “*a priori*.” Concerning the macroscopic dielectric constant, the use of the GGA was found to yield very little improvement with respect to LDA.¹³ Whether GGA definitely represents a systematic improvement over LDA is hence still unclear.

In the approach considered here, we choose a different scheme to overcome the LDA.²⁸ Reproposing an idea contained in the original work of Kohn and Sham,³ we use an energy functional appropriate for systems with small variations of the density (“almost constant density” regime). This functional, in the following indicated as nonlocal density approximation (NLDA), considers nonlocal density contributions through the exchange-correlation kernel of the homogeneous electronic gas, and in the limit for an homogeneous system yields the exchange-correlation energy of the homogeneous electron gas. In the NLDA approximation there is no limitation on the gradient of the density.

As in Ref. 29, we use the NLDA functional both to construct the pseudopotential for the element under consideration, and to calculate the geometry (lattice parameter) and the electronic structure of the solid. In the present paper, we focus on the case of silicon. We include local-field effects in the dielectric screening by considering the long-wavelength limit of the $\mathbf{G}=\mathbf{G}'=0$ element of the inverse dielectric matrix;³⁰ the effect of the nonlocality of the pseudopotential^{6,31,32} is also included. The NLDA dielectric constant is then compared with LDA as well as GGA values. As a result, within NLDA the dielectric constant undergoes a reduction with respect to the LDA value, bringing the overestimate of the experimental value from 13% to 9%.

We have also considered the effects induced on the linear optical response by using the NLDA scheme to treat the exchange-correlation effects. To this purpose, we show the computed NLDA absorption spectrum, and compare it with the random phase approximation (RPA) and LDA ones.

Finally, since exchange-correlation effects beyond the LDA are likely to become more relevant at finite q vectors, we have also calculated NLDA electron energy-loss spectra and dynamic structure factors at q vectors of the order of, and larger than, the Fermi wave vector. The spectra are compared with electron-energy-loss spectroscopy (EELS) and inelastic x-ray scattering spectroscopy (IXSS) experimental data as well as with RPA and LDA results.

II. NLDA APPROXIMATION FOR THE EXCHANGE-CORRELATION FUNCTIONAL

In the local-density approximation the exchange-correlation term of the energy functional is written as

$$E_{xc}^{\text{LDA}}[\rho] = \int d^3r \rho(\mathbf{r}) e_{xc}^{\text{HEG}}[\rho(\mathbf{r})], \quad (1)$$

where $e_{xc}^{\text{HEG}}(\rho)$ is the exchange-correlation energy per particle of the homogeneous electron gas at density ρ .

Analytical parameterizations of the function $e_{xc}^{\text{HEG}}(\rho)$, which are of practical and common use in actual LDA calculations, are available since 1971. They are based on accurate results for the homogeneous electron gas, obtained either within the many-body theory,³³ or by performing explicit

quantum Monte Carlo calculations.^{34,35} According to Eq. (1), the exchange-correlation potential $V_{xc}[\rho](\mathbf{r})$, defined as $\delta E_{xc}/\delta\rho$, takes the form

$$V_{xc}^{\text{LDA}}[\rho](\mathbf{r}) = e_{xc}^{\text{HEG}}[\rho(\mathbf{r})] + \rho(\mathbf{r}) \left. \frac{de_{xc}^{\text{HEG}}}{d\rho} \right|_{\rho(\mathbf{r})}. \quad (2)$$

In LDA, hence, the xc potential at point \mathbf{r} depends only on the value of the electron density at the same point \mathbf{r} , and is not influenced by any change of the density at points \mathbf{r}' different from \mathbf{r} . This is reflected in the fact that the exchange-correlation kernel, defined as

$$K_{xc}[\rho](\mathbf{r}, \mathbf{r}') = \frac{\delta E_{xc}}{\delta\rho(\mathbf{r})\delta\rho(\mathbf{r}')} = \frac{\delta V_{xc}(\mathbf{r})}{\delta\rho(\mathbf{r}')}, \quad (3)$$

is proportional to a δ function

$$K_{xc}^{\text{LDA}}[\rho](\mathbf{r}, \mathbf{r}') = \delta(\mathbf{r}, \mathbf{r}') \left. \frac{dV_{xc}^{\text{LDA}}}{d\rho} \right|_{\rho=\rho(\mathbf{r})}. \quad (4)$$

However, expression (4) depends on the assumed approximation (1), and even for the homogeneous electron gas it is *not* exact, at variance with Eqs. (1) and (2). Actually, the Fourier transform of the $K_{xc}[\rho](\mathbf{r}, \mathbf{r}')$ of the homogeneous electron gas has been recently computed with quantum Monte Carlo for several values of q and ρ .³⁶ Assuming the expression (4) for K_{xc}^{HEG} is equivalent to approximate the q -dependent Fourier transform of the xc kernel of the homogeneous electron gas with its $q=0$ value.

A possible way to go beyond the LDA is the generalized gradient approximation (GGA), which includes the lowest-order density-gradient corrections. The GGA exchange-correlation energy functional is

$$E_{xc}^{\text{GGA}}[\rho] = E_{xc}^{\text{LDA}}[\rho] + \int d^3r c(\rho(\mathbf{r})) \frac{|\nabla\rho(\mathbf{r})|^2}{\rho^{4/3}(\mathbf{r})}, \quad (5)$$

where $c(\rho(\mathbf{r}))$ is a function of the density, which, in analogy with e_{xc}^{HEG} , has been parametrized in suitable forms. The corresponding approximation for the $K_{xc}(q)$ of the homogeneous electron gas includes terms up to second order in q , i.e.,

$$K_{xc}^{\text{GGA}}(\mathbf{q}) = K_{xc}^{\text{LDA}} + bq^2. \quad (6)$$

This approximation is clearly a good one for systems of slowly varying density; however, in real systems (like atoms, molecules, and solids), it has been shown to improve only partially with respect to LDA. In fact, GGA gives an improvement on the LDA cohesive energies, but sometime worsens the LDA results for other quantities as the lattice constants or the bulk moduli.^{23–27}

As it was shown already by Kohn and Sham in their seminal work on DFT,³ it is possible to consider a different limit than that of a vanishing gradient: namely, by considering a system characterized by

$$\rho(\mathbf{r}) = \rho_0 + \Delta\rho(\mathbf{r}), \quad (7)$$

with

$$\int d^3r \Delta\rho(\mathbf{r}) = 0, \quad (8)$$

and

$$|\Delta\rho(\mathbf{r})/\rho_0| \ll 1 \quad (9)$$

(“almost constant density” regime), Hohenberg-Kohn (HK) have shown that it is possible to partially resum the gradient expansion to all orders, obtaining, to the lowest order in $\Delta\rho$ (Refs. 2 and 3)

$$E_{xc}[\rho] \approx E_{xc}^{\text{HEG}}(\rho_0) - \frac{1}{4} \int d^3r d^3r' K_{xc}^{\text{HEG}}(\rho_0; |\mathbf{r} - \mathbf{r}'|) \times [\rho(\mathbf{r}) - \rho(\mathbf{r}')]^2, \quad (10)$$

where $K_{xc}^{\text{HEG}}(\rho_0; |\mathbf{r} - \mathbf{r}'|)$ is the exchange-correlation kernel of the homogeneous electron gas with density ρ_0 .

Recently, it has been shown by some of us^{28,29} that an expression similar to Eq. (10) can be derived from a functional expansion of V_{xc} , avoiding to introduce gradient expansions and their resummation. The expression for $E_{xc}[\rho]$ derived in Refs. 28 and 29 reads

$$E_{xc}[\rho] \approx E_{xc}^{\text{LDA}}[\rho] - \frac{1}{4} \int d^3r d^3r' K_{xc}^{\text{HEG}}(\bar{\rho}; |\mathbf{r} - \mathbf{r}'|) \times [\rho(\mathbf{r}) - \rho(\mathbf{r}')]^2, \quad (11)$$

where K_{xc}^{HEG} is taken at a density $\bar{\rho}$ intermediate between $\rho(\mathbf{r})$ and $\rho(\mathbf{r}')$. Expression (11) reduces to the LDA if the differences $[\rho(\mathbf{r}) - \rho(\mathbf{r}')]$ can be neglected for every $(\mathbf{r}, \mathbf{r}')$ pair such that $|\mathbf{r}' - \mathbf{r}| < \Delta r$, where Δr is the spatial range over which K_{xc} extends.

To be applied to real inhomogeneous systems this scheme requires a knowledge of $K_{xc}(\bar{\rho}; |\mathbf{r} - \mathbf{r}'|)$. In the same spirit of what has been done in the case of the LDA, one can exploit the results of the accurate quantum Monte Carlo calculations of $K_{xc}^{\text{HEG}}(\rho; q)$.³⁶ In fact, the K_{xc} of the homogeneous electron gas (HEG) is related to the so-called local-field factor $G(q)$ by the relation

$$K_{xc}^{\text{HEG}}(q) = -\frac{4\pi}{q^2} G(q). \quad (12)$$

There are various parametrization of the (static) $G(q)$ for the homogeneous electron gas, both theoretical and interpolated from Monte Carlo data: from the early form of Hubbard to the more refined Utsumi-Ichimarū expression,³⁷ to recent quantum Monte Carlo (QMC) calculations.³⁶ In this paper, we have used everywhere the form given in Ref. 38, which is a parametrization of the QMC data of Moroni, Ceperley, and Senatore.³⁶ In this expression

$$G(q) = CQ^2 + \frac{BQ^2}{g + Q^2} + \alpha Q^4 e^{-\beta Q^2}, \quad Q = q/k_F, \quad (13)$$

we recognize a Lorentzian Hubbard-like term, plus a Gaussian term that allows to reproduce quantitatively the numerical data of Ref. 36. C, B, g, α , and β are functions of the density.³⁸

In this case, the resulting V_{xc} at point \mathbf{r} includes nonlocal contributions from the density at all the points \mathbf{r}' over which $\rho(\mathbf{r})$ differs from $\rho(\mathbf{r}')$, and $K_{xc}^{\text{HEG}}(\bar{\rho}; |\mathbf{r} - \mathbf{r}'|)$ differs from 0. Still, there is an arbitrariness in the choice of the density argument $\bar{\rho}$ to be put in K_{xc}^{HEG} : in principle, both $\rho(\mathbf{r}), \rho(\mathbf{r}')$, or any combination of them can be used, if the exchange-correlation potential is to be determined to first order in the density variations. On the other hand, one hopes that a suitable choice of $\bar{\rho}$ could improve the performance of the functional in strongly inhomogeneous systems. This fact has been thoroughly discussed by Gunnarsson, Jonson, and Lundqvist in 1979;³⁹ in particular, they demonstrated that some choice, as the one

$$\bar{\rho} = \rho[\tfrac{1}{2}(\mathbf{r} + \mathbf{r}')] \quad (14)$$

can even lead to divergent E_{xc} , in the case of strongly inhomogeneous systems as atoms and jellium surfaces. The difficulties in determining a unique choice for the density argument in K_{xc}^{HEG} hindered further efforts toward a practical use of this NLDA functional.

The derivation given in Ref. 29 suggests to take

$$\bar{\rho} = \tfrac{1}{2}[\rho(\mathbf{r}) + \rho(\mathbf{r}')]. \quad (15)$$

This choice was also considered by the authors of Ref. 39, as one of the possible choices which cannot give divergent results; in Ref. 29 it is suggested as the most natural one. Moreover, in the case of silicon, whose electronic density is not strongly inhomogeneous, it has been shown that the choice of $\bar{\rho}$ does not affect significantly the total energy and the electronic structure.²⁹

III. NLDA DIELECTRIC MATRIX

Starting from the structural properties and electronic states consistently obtained within NLDA for bulk silicon, we obtain the dielectric response using the perturbative time-dependent DFT approach.⁴⁰ Local-field effects are included in the standard Adler-Wiser way.³⁰ In the following, we illustrate the way used to compute NLDA exchange-correlation contributions in the calculation of the dielectric function.

We consider the *test-particle* inverse dielectric matrix ε^{-1} , i.e., the dielectric response of the system to a classical probe, so that exchange-correlation effects between the test particle and the system are excluded. The test-particle inverse dielectric matrix is related to the polarizability χ through^{7,41}

$$\varepsilon^{-1} = 1 + V_C \chi, \quad (16)$$

where matrix notation has been adopted, so that products must be intended as convolutions in real space, or matrix products in reciprocal space. V_C is the Coulomb potential. The polarizability χ is related to the independent particle polarizability, χ_{KS} , through the relation^{7,41}

$$\chi = (1 - \chi_{KS} V_C - \chi_{KS} K_{xc})^{-1} \chi_{KS}. \quad (17)$$

Substituting Eq. (17) in Eq. (16), we get the expression of the inverse dielectric matrix in term of χ_{KS} and K_{xc}

$$\varepsilon^{-1} = 1 + V_C(1 - \chi_{KS}V_C - \chi_{KS}K_{xc})^{-1}\chi_{KS}. \quad (18)$$

Hence, the key quantities entering the calculation of the inverse dielectric matrix are χ_{KS} and K_{xc} . Neglecting K_{xc} , the dielectric matrix reduces to the usual RPA form

$$\varepsilon^{\text{RPA}} = 1 - V_C\chi_{KS}. \quad (19)$$

Application of first-order perturbation theory to the effective one-particle Kohn-Sham equation yields the standard Adler-Wiser³⁰ result for χ_{KS} (atomic units are used throughout)

$$\begin{aligned} \chi_{\mathbf{G}\mathbf{G}'}^{\text{KS}}(\mathbf{q}, \omega) &= \frac{2}{\Omega} \sum_{n, n', \mathbf{k}} \langle n', \mathbf{k} | e^{-i(\mathbf{q}+\mathbf{G})\mathbf{r}} | n, \mathbf{k} + \mathbf{q} \rangle \langle n, \mathbf{k} + \mathbf{q} | \\ &\times e^{i(\mathbf{q}+\mathbf{G}')\mathbf{r}'} | n', \mathbf{k} \rangle \cdot \frac{f(\varepsilon_{n, \mathbf{k}+\mathbf{q}}) - f(\varepsilon_{n', \mathbf{k}})}{\varepsilon_{n', \mathbf{k}} - \varepsilon_{n, \mathbf{k}+\mathbf{q}} + \omega + i\eta}, \end{aligned} \quad (20)$$

where n and n' are summed over all the bands at the point in the reciprocal space \mathbf{k} , and \mathbf{k} is summed over the first Brillouin zone. f is the Fermi-Dirac distribution function and $|n, \mathbf{k}\rangle$ and $\varepsilon_{n, \mathbf{k}}$ are the Kohn-Sham set of one-electron wave functions and eigenvalues. Ω is the crystal volume.

In order to compute Eq. (17), we need the exchange-correlation kernel. In the LDA approximation one has

$$K_{xc}^{\text{LDA}}(\mathbf{q}) = B(\mathbf{G} - \mathbf{G}'). \quad (21)$$

As we pointed out previously, the constant behavior with respect to q is incorrect, even in the homogeneous electron gas. In our NLDA approach, we use the xc kernel of the homogeneous electron gas $K_{xc}^{\text{HEG}}(\bar{\rho}; |\mathbf{r} - \mathbf{r}'|, \omega)$, calculated at the density $\bar{\rho}$ given by Eq. (15), consistently with what we do in the calculation of the DFT electronic structure

$$K_{xc}^{\text{NLDA}}(\mathbf{r}, \mathbf{r}', \omega) = K_{xc}^{\text{HEG}}\left[\frac{\rho(\mathbf{r}) + \rho(\mathbf{r}')}{2}; |\mathbf{r} - \mathbf{r}'|, \omega\right]. \quad (22)$$

The NLDA K_{xc} is truly nonlocal, and its reciprocal space expression is now q dependent. However, the $K_{xc}(q)$ considered in Eqs. (10) and (12) is static, i.e., it is only relevant for $\omega = 0$, while the polarizability χ in Eq. (19) is ω dependent. In principle, the $K_{xc}(q)$ appearing in Eqs. (16) and (17) is also an ω -dependent quantity.

The ω dependence of $K_{xc}(q)$ could be included following the parametrization given by Gross and Kohn⁴¹ (GK) in the $q \rightarrow 0$ limit, as well as the more general expression by Dabrowski⁴² that extends the GK result to finite q . As pointed out by GK,⁴¹ however, neglecting the frequency dependence of K_{xc}^{HEG} (i.e., working within the adiabatic approximation) does not introduce significant errors. In any case, it will not affect the static response, which is the main concern of this paper. Hence, we neglect the ω dependence, i.e., we take

$$K_{xc}^{\text{HEG}}(\rho; |\mathbf{r} - \mathbf{r}'|, \omega) \approx K_{xc}^{\text{HEG}}(\rho; |\mathbf{r} - \mathbf{r}'|, 0). \quad (23)$$

Our NLDA exchange-correlation kernel can be expressed in reciprocal space as

$$K_{xc}^{\text{NLDA}}(\mathbf{q}) = \sum_{\mathbf{G}''} \tilde{K}_{xc}^{\text{HEG}}(\mathbf{G} - \mathbf{G}'', \mathbf{G}' - \mathbf{G}''; |\mathbf{q} + \mathbf{G}''|), \quad (24)$$

where with $\tilde{K}_{xc}^{\text{HEG}}$ we indicate the Fourier transform of $K_{xc}^{\text{HEG}}(\bar{\rho}; q)$ with respect to the space variables \mathbf{r} and \mathbf{r}' on which it depends through the density argument $\bar{\rho}$:

$$\begin{aligned} K_{xc}^{\text{HEG}}\left[\frac{\rho(\mathbf{r}) + \rho(\mathbf{r}')}{2}; q\right] \\ = \sum_{\mathbf{G}_1, \mathbf{G}_2} e^{i\mathbf{G}_1\mathbf{r}} e^{-i\mathbf{G}_2\mathbf{r}'} \tilde{K}_{xc}^{\text{HEG}}(\mathbf{G}_1, \mathbf{G}_2; q). \end{aligned} \quad (25)$$

Details of the derivation of Eq. (24) are reported in Appendix A.

We use then $K_{xc}^{\text{NLDA}}(\mathbf{q})$ in the calculation of the macroscopic dielectric function, defined as

$$\varepsilon_{\text{M}}(\mathbf{q}, \omega) = 1/\varepsilon_{\mathbf{0}\mathbf{0}}^{-1}(\mathbf{q}, \omega), \quad (26)$$

and, in particular, to obtain the macroscopic dielectric constant

$$\varepsilon_{\text{M}} = \lim_{q \rightarrow 0} 1/\varepsilon_{\mathbf{0}\mathbf{0}}^{-1}(\mathbf{q}, \omega = 0). \quad (27)$$

In general, the macroscopic dielectric constant is different from $\varepsilon_{\mathbf{0}\mathbf{0}}(\mathbf{q} \rightarrow 0, \omega = 0)$, due to the presence of nonzero off-diagonal elements in the dielectric matrix, which are related to the so-called *local-field* effects. In fact, the relation

$$\delta V_{\text{tot}}(\mathbf{q} + \mathbf{G}, \omega) = \sum_{\mathbf{G}'} \varepsilon_{\mathbf{G}\mathbf{G}'}^{-1}(\mathbf{q}, \omega) \delta V_{\text{ext}}(\mathbf{q} + \mathbf{G}', \omega) \quad (28)$$

shows that if the dielectric matrix has nonzero off-diagonal elements, in the total screened potential δV_{tot} there are Fourier components at wave vectors $\mathbf{q} + \mathbf{G}$ that differ by reciprocal lattice vectors from those of the external field δV_{ext} . In direct space, this corresponds to the presence of microscopic fluctuations in the induced field, explaining the name of *local-field* effects. In semiconductors, local-field effects are able to change also the macroscopic dielectric constant by as much as 10-20 %, ⁸ so that they cannot be neglected.

IV. SILICON CALCULATION

The first step of our calculation is a fully self-consistent ground-state calculation for bulk silicon, using the NLDA xc energy functional. In the LDA exchange-correlation term of the functional we use the interpolation formula of Perdew and Zunger³⁵ derived from Monte Carlo data of Ceperley and Alder.³⁴ The exchange-correlation kernel K_{xc} used in the second term of Eq. (10) is the analytic formula for the homogeneous electron gas,³⁸ fitted to the data of Ref. 36.

We generate *ab initio* normconserving pseudopotentials using the Martins and Troullier scheme.⁴³ Besides a standard LDA pseudopotential, used for the LDA and RPA dielectric function calculations, we generate also a NLDA pseudopotential (i.e., including the NLDA corrections to the xc energy functional throughout all the atomic calculations), to be fully consistent within our scheme. The fully separable Kleinman-Bylander representation⁴⁴ is used throughout. We employ a

TABLE I. Convergence of the RPA ϵ_M with respect to the number of special points in the IBZ.

Number of k points	ϵ_M^{RPA}
10	13.06
28	12.24
60	12.20

plane-waves basis set, with a cutoff of 18 Ry on the kinetic energy (corresponding to about 300 plane waves at a general point in the Brillouin zone).

The computed NLDA lattice parameter is 10.18 a.u. Compared with our LDA computed value of 10.16, we obtain a slight improvement toward the experimental value (10.26). The bulk modulus decreases from 0.98 to 0.95 Mbar. A more detailed discussion of the behavior of NLDA with respect to ground-state properties other than the dielectric constant for a wide range of materials is given in Ref. 29. The self-consistent NLDA electronic structure is used as an input for the calculation of the dielectric matrix. With respect to LDA, NLDA bands show a slight opening of the gaps, of the order of 0.1 eV.

The independent-electron polarizability χ_{KS} is evaluated from Eq. (20), taking special care of the nonanalytic portion of the matrix in the case of the limit for $q \rightarrow 0$. This limit is performed using first-order perturbation theory for the wave functions at point $\mathbf{k} + \mathbf{q}$, and carefully treating the nonlocal parts of the external potential contained in the pseudopotentials.⁷

The small \mathbf{q} vector used in the calculation is approximately equal to 1/10000 of the Brillouin zone, and is taken along a direction that avoids the symmetries of the system. Further details about the $q \rightarrow 0$ limit are given in Appendix B.

The Brillouin zone integration involved in Eq. (20) is done using 10, 28, and 60 special points of the Monkhorst and Pack type⁴⁵ in the irreducible Brillouin zone (IBZ). The 28 k points set yields results converged within 1%, as shown in Table I, where we give the values of the RPA dielectric constant obtained with the different sets of k points.

We have carefully verified the convergence with respect to the number of plane waves, and to the number of empty (conduction) bands included (Tables II and III). For the energy cutoff we find, consistently with the existing literature, that 169 plane waves are enough; we include 66 conduction bands, even if our calculations suggest that the static dielectric constant is already converged using 26 empty bands.

TABLE II. Convergence of the RPA ϵ_M with respect to the dimension of the dielectric matrix.

Number of plane waves in ϵ and χ	ϵ_M^{RPA}
27	12.67
59	12.44
89	12.33
169	12.24
181	12.22
259	12.18
307	12.17

TABLE III. Convergence of the RPA ϵ_M with respect to the number of bands used.

Number of bands	ϵ_M^{RPA}
15	12.148
30	12.207
50	12.227
70	12.235
168	12.239
200	12.239

V. RESULTS

A. The static dielectric constant

Our results for the dielectric constant both in RPA, LDA, and NLDA, with and without local-fields effects, are reported in Table IV. First of all we notice that, in agreement with previous calculations, local-field effects reduce ϵ_M by 10-20 %. Another considerable reduction is due to the proper inclusion of the contribution due to nonlocal terms in the external potential, in the long-wavelength limit (see Appendix B). On the contrary, the inclusion of xc effects beyond RPA through an LDA exchange-correlation kernel (K_{xc}^{LDA}) increases the dielectric constant, both with and without local-field effects. Replacing the LDA kernel with the NLDA one yields a reduction of the dielectric constant of about 3% ($\epsilon_M^{\text{NLDA}} = 12.5$).

To explicitly demonstrate that this improvement is not simply due to the fact that NLDA gives a slightly larger equilibrium lattice constant (10.18 a.u.), we performed the calculation of the NLDA dielectric constant also at the LDA lattice constant (10.16 a.u.). The resulting value (12.50 instead of 12.51) is changed only by one part over 10^3 .

In Table V, we compare our computed values of the dielectric constant with those obtained by other authors. Our RPA and LDA values coincide with those reported by Hybertsen and Louie,⁷ who used the same scheme. To compare with the values obtained in other calculations, we need to critically consider the parameters that mainly affect the results, particularly the lattice constant, and the pseudopotentials used. We choose to always use the theoretical equilibrium lattice constant, in the same spirit of the authors of Ref. 13. This choice is dictated by the concern of a completely *ab initio* picture and by the consideration that using a nonequilibrium (e.g., experimental) lattice constant would correspond to introduce an external constraint (i.e., pressure) in

TABLE IV. Calculated values of the static dielectric constant ϵ_M in the three approximations considered in the present work; first column: neglecting local-field effects; second column: neglecting contributions due to nonlocal terms in the external potential; third column: considering local-field effects and contributions due to non-local terms in the external potential.

	NLF	NNL	LF+NL
RPA	13.6	14.2	12.2
LDA	15.4	15.0	12.9
NLDA	14.9	14.5	12.5

TABLE V. Electronic dielectric constant of Si as calculated by different authors; GGA refers to the gradient corrected results of Ref. 13.

	a_0 (a.u.)	ϵ_M
RPA, present work	10.16	12.2
LDA, present work	10.16	12.9
NLDA, present work	10.18	12.5
Hybertsen-Louie (Ref. 7), RPA		12.2
Hybertsen-Louie (Ref. 7), LDA		12.9
Baroni-Resta (Ref. 6), RPA	10.20?	12.0
Baroni-Resta (Ref. 6), LDA	10.20	12.7
Dal Corso–Baroni-Resta (Ref. 13), GGA	10.38	12.6
Gavrilenko-Bechstedt (Ref. 8), RPA	10.23	11.8
Gavrilenko-Bechstedt (Ref. 8), LDA	10.23	12.7
Levine-Allan (Ref. 12), LDA	10.26	13.5
Levine-Allan (Ref. 12), GW	10.26	11.2
Experimental (Ref. 49)	10.26	11.4

our theoretical description. This is perhaps influent in silicon, when only the electronic properties are considered, but is known to lead to large errors when the ionic degrees of freedom are of interest (e.g., phonon, elastic constants, etc.). Results for ϵ_M are reported in Table V. We notice that Baroni and Resta⁶ obtained a slightly different LDA dielectric constant (12.7) and a lattice constant closer to the experiment (10.20 a.u.) than ours. The GGA of Dal Corso–Baroni-Resta,¹³ on the other hand, represents only a slight improvement with respect to their LDA value, obtained using the same scheme. In fact, the GGA yields $\epsilon_M = 12.6$, compared to the LDA value of 12.7. Actually, a larger reduction arising directly from the GGA correction is almost completely canceled by the use of the (overestimated) GGA lattice constant. In this way, the NLDA improvement can be considered larger than that of the GGA, even though in the actual calculations they both reach about the same absolute value.

The present results, as those of Ref. 13, suggest that, even beyond the LDA, DFT cannot account completely for the experimental macroscopic dielectric constant. The NLDA has been shown to reduce slightly the mismatch between experimental and theoretical values, but the error remains large, compared to the performances obtained by DFT in the prediction of other ground-state observables.

Errors due to the core electrons contribution, in the case of silicon, are likely to be very small. Hence, it seems that the large overestimation of ϵ_M encountered in LDA as well as in nonlocal corrected schemes—the GGA or the present NLDA—should be explained by the inadequacy of DFT in describing a real infinite, nonmetallic, periodic system under the influence of an electric field. As stated in Ref. 9, a polarization dependence in the xc functional should be introduced, in order to extend the validity of the Kohn-Sham theorem to such a system. The fact that nonlocal corrections as GGA or NLDA are not sufficient to correct the failure of LDA can be understood also in connection with the behavior of the exchange-correlation kernel K_{xc} in the $q \rightarrow 0$ limit. In fact, this limit remains finite, and coincident with the LDA constant value, both in the GGA and NLDA schemes. On the other hand, in the expression for the dielectric matrix [Eq.

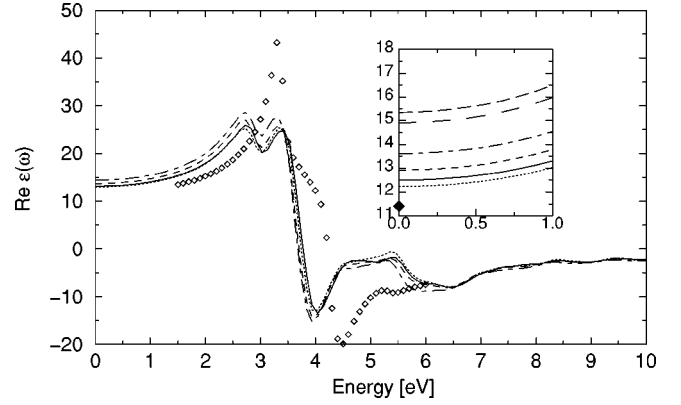


FIG. 1. Real part of the macroscopic dielectric function. Open diamonds: experimental values of Aspnes and Studna (Ref. 50); dotted, short-dashed, and solid lines represent RPA, LDA, and NLDA results, respectively, always including the local field effects. The dashed-dotted line represents the RPA curve neglecting local-field effects. The theoretical curves are calculated using 10 k points in the IBZ, 169 plane waves, and 70 bands; a broadening of 0.25 eV has been superimposed. In the inset, that refers to the low-frequency limit, we used 28 k points and a negligible broadening (0.001 eV). The effects of the neglect of local-field effects are also shown for the LDA curve (medium-dashed line) and for the NLDA (long-dashed line) in the inset.

18] K_{xc} appears only in products with χ_{KS} , whose $\mathbf{G}=0$ or $\mathbf{G}'=0$ elements go to zero for $q \rightarrow 0$. Hence, no corrections to ϵ_M can come directly through the “head” ($\mathbf{G}=\mathbf{G}'=0$ element) or through the “wings” ($\mathbf{G}=0$ or $\mathbf{G}'=0$ elements) of the K_{xc} matrix, unless they diverge for $q \rightarrow 0$. In fact, a $1/q^2$ divergence of the second derivative of the exchange-correlation energy is predicted in the case of a density-polarization functional theory.¹¹ This divergence is related to the presence of a finite gap, and should be present in any periodic, infinite, nonmetallic system. However, it is completely absent in the K_{xc} expressions usually employed within DFT, and derived from the homogeneous electron gas.

B. Optical and energy-loss spectra

Using time-dependent density-functional theory according to the formulation given by Runge and Gross,⁴⁰ and applying the Gross and Kohn adiabatic approximation,⁴¹ we calculate the ω -dependent macroscopic dielectric function in the three considered approximations (RPA, LDA, and NLDA), at $q=0$ and at finite q . It should be specified that the dynamic behavior of the dielectric function, yielding optical absorption and energy-loss spectra, cannot be directly extracted from the time-dependent local-density approximation (TD-LDA), where quasiparticle and excitonic effects are neglected. However, our interest in this case is to compare NLDA spectra with the LDA ones, in order to analyze if differences in the shape of the spectra appear. They can be expected, *a priori*, to be of the same size as the slight improvement registered for the value of the dielectric constant.

In Fig. 1, we plot the real part of the dielectric function in the $q \rightarrow 0$ limit for the three cases of RPA, adiabatic LDA and NLDA, both considering and neglecting the local-field effects. In the inset, the low-frequency (static) limits are

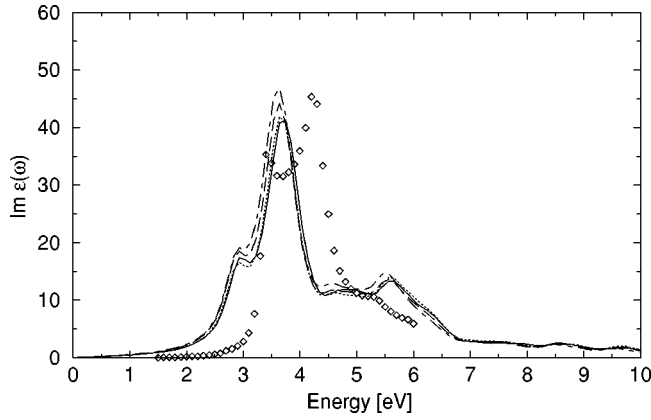


FIG. 2. Imaginary part of the macroscopic dielectric function. Diamonds: experimental values of Aspnes and Studna (Ref. 50); dotted line: RPA; dashed line: LDA; solid line: NLDA; dashed-dotted line: RPA neglecting local-field effects. A broadening of 0.25 eV has been superimposed on the theoretical curves.

shown. Clearly, local-field effects appear to influence in a relevant way the resulting spectra. However, xc effects are minor, as no appreciable differences appear between the shapes of RPA, LDA, and NLDA spectra.

A similar conclusion can be drawn for the absorption spectra, i.e., for the imaginary part of the dielectric function (Fig. 2). At finite q (i.e., away from the $q \rightarrow 0$ limit), more remarkable differences between RPA, LDA, and NLDA spectra appear. A comparison of the computed imaginary part of the inverse dielectric function with the EELS spectra measured by Stiebling⁴⁶ shows that the inclusion of xc effects (i.e., using LDA or NLDA) considerably improves RPA spectra (Fig. 3). However, the differences between the LDA and the NLDA cases are still very small. This is due to the fact that the NLDA exchange-correlation kernel for small q tends to the constant value of the LDA xc kernel. At larger q values, i.e., for $q \approx k_F$, we have considered the dynamic structure factor, $S(\mathbf{k}, \omega)$, which is directly related to the inverse dielectric matrix,

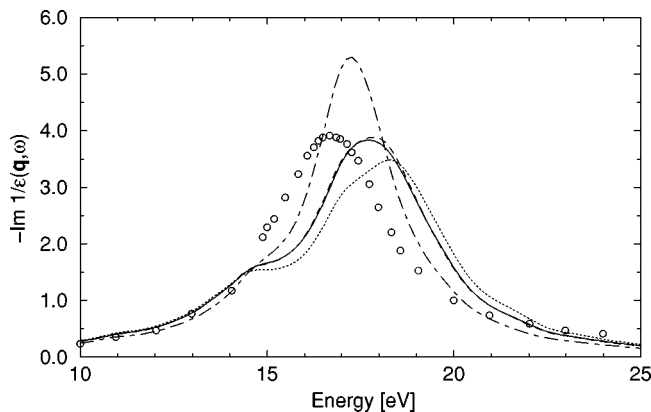


FIG. 3. Imaginary part of ε^{-1} . Circles: experimental energy loss spectra of Stiebling (Ref. 46); dotted line: RPA; dashed line: LDA; solid line: NLDA; dashed-dotted line: RPA neglecting local-field effects. Theoretical spectra are calculated at $\mathbf{q} = (0, 0.047, 0.047)2\pi/a$, corresponding to the experimental value; a broadening of 0.75 eV has been used in all the theoretical spectra.

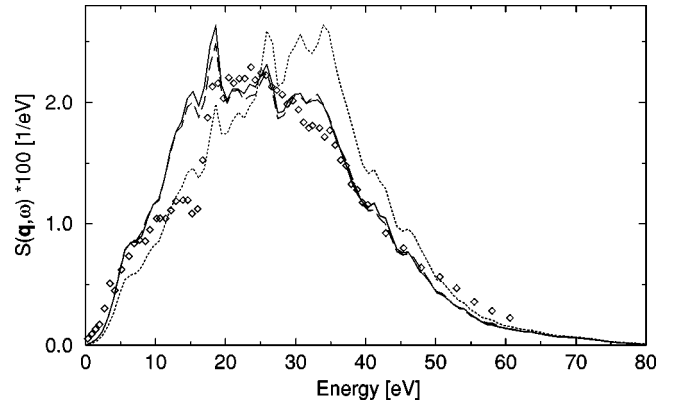


FIG. 4. Dynamic structure factor $S(\mathbf{q}, \omega)$ (see text). Diamonds: experimental inelastic x-ray scattering spectroscopy spectra of Sturm, Schülke and Schmitz (Ref. 47); dotted line: RPA; dashed line: LDA; solid line: NLDA. Both experimental and theoretical data are taken at $q = 1.25$ a.u. in the $[111]$ direction; we used 28 k points in the IBZ, and a broadening of 0.5 eV in the calculation of the theoretical spectra.

$$S(\mathbf{q} + \mathbf{G}, \omega) = -\frac{|\mathbf{q} + \mathbf{G}|}{4\pi^2} \text{Im} \varepsilon_{\mathbf{G}\mathbf{G}}^{-1}(\mathbf{q}, \omega). \quad (29)$$

$S(\mathbf{k}, \omega)$ is measured in inelastic x-ray scattering spectroscopy (IXSS) experiments.⁴⁷ Again, no appreciable differences between LDA and NLDA appear, even at $q \approx k_F$ (Fig. 4). This can be explained considering the form of $K_{xc}(q)$ used in our calculation: as shown in Fig. 2 of Ref. 38, for $q \approx k_F$ our K_{xc} recovers a value very similar to the $q = 0$ one.

Only at very large q , i.e., at $q \approx 3k_F$, larger differences begin to appear (Fig. 5). The situation is now reversed, i.e., the LDA spectrum strictly resembles the RPA one, while the NLDA spectrum shows slight differences in the shape. However, no experimental data is available at these high-transferred momenta.

VI. CONCLUSIONS

We calculated the dielectric function of silicon within and beyond the local-density approximation scheme. All the ingredients of the calculation, i.e., the pseudopotential, band structure, lattice constant, etc. were determined consistently

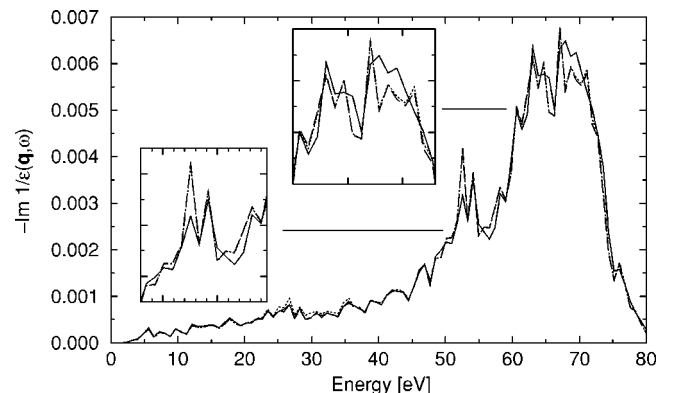


FIG. 5. Imaginary part of ε^{-1} . Dotted line: RPA; dashed line: LDA; solid line: NLDA. q is 3.40 a.u. along the $[111]$ direction; we used 28 k points in the IBZ, and a broadening of 0.1 eV.

with the choice of the xc kernel. We found very small changes of the spectral properties determined by non-LDA effects. For the static macroscopic dielectric constant, which is the main concern here, we found a value of 12.5, to be compared with the LDA value of 12.9. Hence, effects beyond the LDA reduce the discrepancy of the LDA calculation of ϵ_M with respect to the experimental value (11.4), but a 9% discrepancy still remains. In view of the well converged and mutually consistent ingredients of our calculation, and of the fact that the choice of $\bar{\rho}$ has proved not to be crucial in silicon,²⁹ we believe the resulting value for its dielectric constant, 12.5, to be close to the best estimate that can be obtained using an xc kernel derived from the homogeneous electron gas. We attribute the residual discrepancy to the neglected long-range tail of K_{xc} , present in all non-metallic, periodic systems, and related to the polarization dependence of the xc kernel.

VII. ACKNOWLEDGMENTS

Useful discussions with Lucia Reining and Rex Godby are gratefully acknowledged. This work has been supported in part by the Italian Ministry of University and Scientific Research (MURST-COFIN 97). Part of the numerical calculations involved in this work have been done at the Inter-university Consortium of the Northeastern Italy for Automatic Computing (CINECA), under the INFM parallel computing initiative. We thank S. Goedecker for providing us an efficient code for fast Fourier transforms.⁴⁸

APPENDIX A: NLDA EXCHANGE-CORRELATION KERNEL

In this appendix, we derive Eq. (24). The notation is restricted to a one-dimensional periodic crystal, since the extension to three dimensions is straightforward. Starting from

$$K_{xc}^{NLDA}(r, r') = K_{xc}^{HEG} \left[\frac{\rho(r) + \rho(r')}{2}; \left| r - r' \right| \right], \quad (A1)$$

we can express $K_{xc}^{NLDA}(r, r')$ in terms of the $K_{xc}^{HEG}(\rho; q)$

$$K_{xc}^{NLDA}(r, r') = \sum_{q', G''} e^{i(q' + G'')(r - r')} \times K_{xc}^{HEG} \left[\frac{\rho(r) + \rho(r')}{2}; \left| q' + G'' \right| \right], \quad (A2)$$

where q' runs inside the first Brillouin zone while G'' is the set of the reciprocal space vectors. Using Eq. (25) we obtain

$$K_{xc}^{NLDA}(r, r') = \sum_{q', G''} \sum_{G_1, G_2} e^{i(q' + G'')(r - r')} e^{iG_1 r} e^{-iG_2 r'} \times \tilde{K}_{xc}^{HEG}(G_1, G_2; |q' + G''|). \quad (A3)$$

The Fourier transform of $K_{xc}^{NLDA}(r, r')$ with respect to r and r' is defined as

$$K_{xcGG'}^{NLDA}(q) = \int dr dr' e^{-i(q+G)r} e^{i(q+G')r'} K_{xc}^{NLDA}(r, r'). \quad (A4)$$

Substituting Eq. (A3) and performing the integration in r and r' we obtain

$$K_{xcGG'}^{NLDA}(q) = \sum_{G''} \tilde{K}_{xc}^{HEG}(G - G'', G' - G''; |q + G''|). \quad (A5)$$

The sum converges quickly, since for large q vectors $K_{xc}^{HEG}(q)$ becomes small, and for large G s the Fourier coefficients of the charge density go to zero exponentially (we verified that in the case of Silicon 89 reciprocal space vectors are enough).

In practical calculations, for every needed \mathbf{q} , we first compute $K_{xc}^{HEG}((\rho(\mathbf{r}) + \rho(\mathbf{r}'))/2; |\mathbf{q} + \mathbf{G}''|)$ for every \mathbf{G}'' , and on a given $(\mathbf{r}, \mathbf{r}')$ mesh. Then, we Fourier transform in order to obtain \tilde{K}_{xc}^{HEG} . Finally, we perform the sum over \mathbf{G}'' , obtaining $K_{xcGG'}^{NLDA}(\mathbf{q})$. The latter is the quantity directly entering the dielectric matrix calculation.

APPENDIX B: CALCULATION OF THE INDEPENDENT-PARTICLE POLARIZABILITY χ_{KS} IN THE LONG-WAVELENGTH LIMIT FOR THE CASE OF FULLY NONLOCAL KLEINMAN-BYLANDER PSEUDOPOTENTIALS

In this appendix we discuss the calculation of $\chi_{KS}(\mathbf{q})$ in the limit for $q \rightarrow 0$ when nonlocal Kleinman-Bylander pseudopotentials are used in the electronic structure calculation.

In Eq. (20) for χ_{KS} , when $q \rightarrow 0$ the matrix elements for $\mathbf{G} = \mathbf{0}$ or $\mathbf{G}' = \mathbf{0}$ (or both) (the ‘‘wings’’ and ‘‘head’’ of the matrix) must be treated with special care. Using perturbation theory, the wave functions at $(\mathbf{k} + \mathbf{q})$ can be obtained in terms of those at \mathbf{k} to first order in \mathbf{q} :

$$\phi_{n, \mathbf{k} + \mathbf{q}}(\mathbf{r}) = e^{i\mathbf{q}\mathbf{r}} \phi_{n, \mathbf{k}}(\mathbf{r}) + \sum_{m \neq n} e^{i\mathbf{q}\mathbf{r}} \phi_{m, \mathbf{k}}(\mathbf{r}) \times \frac{\langle \phi_{m, \mathbf{k}} | -i\mathbf{q}\nabla + [V_{nl}, i\mathbf{q}\mathbf{r}] | \phi_{n, \mathbf{k}} \rangle}{\epsilon_{n, \mathbf{k}} - \epsilon_{m, \mathbf{k}}}, \quad (B1)$$

where the nonlocal part of the ionic pseudopotential, V_{nl} , appears explicitly since it does not commute with local functions of \mathbf{r} .

Substituting Eq. (B1) into Eq. (20), we obtain

$$\chi_{00}^{KS}(\mathbf{q} \rightarrow 0) = \frac{2}{\Omega} \sum_{n, n', \mathbf{k}} \frac{1}{(\epsilon_{n', \mathbf{k}} - \epsilon_{n, \mathbf{k}})^3} \langle n', \mathbf{k} | -i\mathbf{q}\nabla + [V_{nl}, i\mathbf{q}\mathbf{r}] | n, \mathbf{k} \rangle \cdot \langle n', \mathbf{k} | -i\mathbf{q}\nabla + [V_{nl}, i\mathbf{q}\mathbf{r}] | n, \mathbf{k} \rangle. \quad (B2)$$

Hence, the ‘‘head’’ goes to zero as q^2 for $q \rightarrow 0$. Similarly,

$$\chi_{0\mathbf{G}'}^{KS}(\mathbf{q} \rightarrow 0) = -\frac{2}{\Omega} \sum_{n, n', \mathbf{k}} \frac{1}{(\epsilon_{n', \mathbf{k}} - \epsilon_{n, \mathbf{k}})^2} \langle n', \mathbf{k} | -i\mathbf{q}\nabla + [V_{nl}, i\mathbf{q}\mathbf{r}] | n, \mathbf{k} \rangle \cdot \langle n', \mathbf{k} | e^{i\mathbf{G}'\mathbf{r}'} | n, \mathbf{k} \rangle, \quad (B3)$$

i.e., the ‘‘wings’’ goes to zero as q .

The evaluation of the matrix elements of $-i\mathbf{q}\nabla$ is straightforward, yielding

$$\langle n', \mathbf{k} | -i\mathbf{q}\nabla | n, \mathbf{k} \rangle = \mathbf{q} \frac{1}{\pi} \sum_{\mathbf{G}} a_{n', \mathbf{k}}^{*\mathbf{G}} a_{n, \mathbf{k}}^{\mathbf{G}}(\mathbf{k} + \mathbf{G}), \quad (\text{B4})$$

where the $a_{n, \mathbf{k}}^{\mathbf{G}}$ are the Fourier coefficients of the Bloch functions

$$\phi_{n, \mathbf{k}}(\mathbf{r}) = \sum_{\mathbf{G}} a_{n, \mathbf{k}}^{\mathbf{G}} e^{-i(\mathbf{k} + \mathbf{G})\mathbf{r}}. \quad (\text{B5})$$

The evaluation of the matrix elements of the commutator $[V_{nl}, i\mathbf{q}\mathbf{r}]$ leads instead to

$$\begin{aligned} \langle n', \mathbf{k} | [V_{nl}, i\mathbf{q}\mathbf{r}] | n, \mathbf{k} \rangle &= \mathbf{q} \sum_{\mathbf{G}\mathbf{G}'} a_{n', \mathbf{k}}^{*\mathbf{G}} a_{n, \mathbf{k}}^{\mathbf{G}'} (\nabla_{\mathbf{K}} + \nabla_{\mathbf{K}'}) \\ &\times V_{nl}(\mathbf{K} + \mathbf{K}'), \end{aligned} \quad (\text{B6})$$

where $\mathbf{K} = \mathbf{k} + \mathbf{G}$ and $\mathbf{K}' = \mathbf{k} + \mathbf{G}'$ and $V_{nl}(\mathbf{K}, \mathbf{K}')$ is the Fourier transform of $V_{nl}(\mathbf{r}, \mathbf{r}')$

$$V_{nl}(\mathbf{K}, \mathbf{K}') = \frac{1}{\Omega} \int d^3r d^3r' e^{-i\mathbf{K}\mathbf{r}} V_{nl}(\mathbf{r}, \mathbf{r}') e^{i\mathbf{K}'\mathbf{r}'}. \quad (\text{B7})$$

In a Kleinman-Bylander scheme,⁴⁴ the nonlocal part of the pseudopotential can be written as

$$V_{nl}^{\text{KB}}(\mathbf{K}, \mathbf{K}') = \sum_s e^{-i(\mathbf{K} - \mathbf{K}')\tau_s} \sum_l P_l(\hat{K}\hat{K}') F_{sl}(K) F_{sl}(K'), \quad (\text{B8})$$

where τ_s are the atomic positions inside the elementary cell, P_l are the Legendre polynomials, and

$$F_{sl}(K) = \sqrt{\frac{4\pi}{\Omega}} (2l+1) K_{sl}(K), \quad (\text{B9})$$

where K_{sl} are the Kleinman-Bylander structure factors⁴⁴

$$K_{sl}(K) = \int dr r^2 \widetilde{\Delta V}_{sl}(r) j_l(Kr) R_l^{\text{PS}}(r). \quad (\text{B10})$$

The final expression is hence

$$\begin{aligned} \langle n', \mathbf{k} | [V_{nl}, i\mathbf{q}\mathbf{r}] | n, \mathbf{k} \rangle &= \mathbf{q} \sum_{\mathbf{G}\mathbf{G}'} a_{n', \mathbf{k}}^{*\mathbf{G}} a_{n, \mathbf{k}}^{\mathbf{G}'} \sum_s e^{-i(\mathbf{K} - \mathbf{K}')\tau_s} \\ &\times \sum_l \left\{ P_l'(\hat{K}\hat{K}') \frac{1}{KK'} \left[\mathbf{K} \left(1 - \frac{\mathbf{K}\mathbf{K}'}{K^2} \right) \right. \right. \\ &+ \left. \left. \mathbf{K}' \left(1 - \frac{\mathbf{K}\mathbf{K}'}{K'^2} \right) \right] F_{sl}(K) F_{sl}(K') + P_l(\hat{K}\hat{K}') \right. \\ &\times \left[\frac{\partial F_{sl}(K)}{\partial K} \right]_{K} F_{sl}(K') \frac{\mathbf{K}}{K} \\ &+ \left. \left. F_{sl}(K) \frac{\partial F_{sl}(K')}{\partial K'} \right]_{K'} \frac{\mathbf{K}'}{K'} \right\}, \end{aligned} \quad (\text{B11})$$

where P_l' are the first derivative of the Legendre polynomials with respect to their argument. From the definition of the Kleinman-Bylander structure factor, the first derivative of the F_{sl} can be expressed analytically

$$F'_{sl}(K) = \sqrt{\frac{4\pi}{\Omega}} (2l+1) \int dr r^3 \widetilde{\Delta V}_{sl}(r) j_l'(Kr) R_l^{\text{PS}}(r), \quad (\text{B12})$$

where the j_l' are the first derivative of the spherical Bessel functions with respect to their argument.

¹R. M. Dreizler and E. K. U. Gross, *Density Functional Theory* (Springer, Berlin, 1990).

²P. Hohenberg and W. Kohn, Phys. Rev. **136**, B864 (1964).

³W. Kohn and L.J. Sham, Phys. Rev. **140**, A1133 (1965).

⁴R. M. Martin, *Festkörperprobleme (Advances in Solid State Physics)*, edited by H.J. Quisser (Pergamon/Vieweg, Braunschweig, 1982), Vol. 25, p. 3.

⁵W. Pickett, Comput. Phys. Rep. **9**, 115 (1989), and references therein.

⁶S. Baroni and R. Resta, Phys. Rev. B **33**, 7017 (1986).

⁷M.S. Hybertsen and S.G. Louie, Phys. Rev. B **35**, 5585 (1987).

⁸V. Gavrilenko and F. Bechstedt, Phys. Rev. B **55**, 4343 (1997).

⁹X. Gonze, Ph. Ghosez, and R.W. Godby, Phys. Rev. Lett. **74**, 4035 (1995).

¹⁰X. Gonze, Ph. Ghosez, and R.W. Godby, Phys. Rev. Lett. **78**, 294 (1997).

¹¹Ph. Ghosez, X. Gonze, and R.W. Godby, Phys. Rev. B **56**, 12 811 (1997).

¹²Z.H. Levine and D.C. Allan, Phys. Rev. B **43**, 4187 (1991).

¹³A. Dal Corso, S. Baroni, and R. Resta, Phys. Rev. B **49**, 5323 (1994).

¹⁴R. Resta, Phys. Rev. Lett. **77**, 2265 (1996).

¹⁵R. Resta, Phys. Rev. Lett. **78**, 2030 (1997).

¹⁶R. Martin and G. Ortiz, Phys. Rev. Lett. **78**, 2028 (1997).

¹⁷R. Martin and G. Ortiz, Phys. Rev. B **56**, 1124 (1997).

¹⁸G. Ortiz, I. Souza, and R. Martin, Phys. Rev. Lett. **80**, 353 (1998).

¹⁹W.G. Aulbur, L. Jönsson, and J.W. Wilkins, Phys. Rev. B **54**, 8540 (1996).

²⁰Another relevant implication of the polarization dependence concerns the $q \rightarrow 0$ asymptotic behavior of the second functional derivative of the exchange-correlation energy with respect to the density (the so-called exchange-correlation kernel K_{xc}). According to Ghosez, Gonze, and Godby, $K_{xc}(q)$ should have a $O(1/q^2)$ divergence for $q \rightarrow 0$, while in DFT it goes to a constant value (the LDA limit). This point is discussed in more detail below.

²¹J. Perdew, K. Burke, and M. Ernzerhof, Phys. Rev. Lett. **77**, 3865 (1996).

²²A. Khein, D.J. Singh, and C.J. Umrigar, Phys. Rev. B **51**, 4105 (1995), and references therein.

²³M. Causa and A. Zupan, Chem. Phys. Lett. **220**, 145 (1994).

²⁴P.H.T. Philipsen and E.J. Baerends, Phys. Rev. B **54**, 5326

- (1996).
- ²⁵A. Dal Corso, A. Pasquarello, A. Baldereschi, and R. Car, Phys. Rev. B **53**, 1180 (1996).
- ²⁶I.H. Lee and R. Martin, Phys. Rev. B **56**, 7197 (1997).
- ²⁷M. Fuchs, M. Bockstedte, E. Pehlke, and M. Scheffler, Phys. Rev. B **57**, 2134 (1998), and references therein.
- ²⁸M. Palumbo, G. Onida, R. Del Sole, and L. Reining, Proceedings of ICPS **XXIII**, edited by M. Scheffler and R. Zimmermann, (World Scientific, Berlin, 1996), p. 609.
- ²⁹M. Palumbo, G. Onida, R. Del Sole, M. Corradini, and L. Reining, Phys. Rev. B **60**, 11 329 (1999).
- ³⁰S.L. Adler, Phys. Rev. **126**, 413 (1962); N. Wiser, *ibid.* **129**, 62 (1963).
- ³¹A.F. Starace, Phys. Rev. A **3**, 1242 (1971).
- ³²R. Del Sole and R. Girlanda, Phys. Rev. B **48**, 11 789 (1993).
- ³³L. Hedin and B.I. Lundqvist, J. Phys. C **4**, 2064 (1971).
- ³⁴D.M. Ceperley and B.I. Alder, Phys. Rev. Lett. **45**, 566 (1980).
- ³⁵J.P. Perdew and A. Zunger, Phys. Rev. B **23**, 5048 (1981).
- ³⁶S. Moroni, D.M. Ceperley, and G. Senatore, Phys. Rev. Lett. **75**, 689 (1995).
- ³⁷S. Ichimaru and K. Utsumi, Phys. Rev. B **24**, 7385 (1981).
- ³⁸M. Corradini, R. Del Sole, G. Onida, and M. Palumbo, Phys. Rev. B **57**, 14 569 (1998).
- ³⁹O. Gunnarsson, M. Jonson, and B.I. Lundqvist, Phys. Rev. B **20**, 3136 (1979).
- ⁴⁰E. Runge and E.K.U. Gross, Phys. Rev. Lett. **52**, 997 (1984).
- ⁴¹E.K.U. Gross and W. Kohn, Phys. Rev. Lett. **26**, 2850 (1985).
- ⁴²B. Dabrowski, Phys. Rev. B **34**, 4989 (1986).
- ⁴³N. Trouiller and J.L. Martins, Phys. Rev. B **43**, 1993 (1991).
- ⁴⁴L. Kleinman and D.M. Bylander, Phys. Rev. Lett. **48**, 1425 (1982).
- ⁴⁵H.J. Monkhorst and J.D. Pack, Phys. Rev. B **13**, 5188 (1976).
- ⁴⁶J. Stiebling, Z. Phys. B **31**, 355 (1978).
- ⁴⁷K. Sturm, W. Schülke, and J.R. Schmitz, Phys. Rev. Lett. **68**, 228 (1992).
- ⁴⁸S. Goedecker, Comput. Phys. Commun. **76**, 294 (1993); S. Goedecker, SIAM (Soc. Ind. Appl. Math.) J. Sci. Stat. Comput. **18**, 1605 (1997).
- ⁴⁹H.H. Li, J. Phys. Chem. Ref. Data **9**, 561 (1980).
- ⁵⁰D.E. Aspnes and A.A. Studna, Phys. Rev. B **27**, 985 (1983).